Ukadike *et al. Mobile DNA* (2023) 14:5
https://doi.org/10.1186/s13100-023-00293-7

Mobile DNA

RESEARCH

Open Access

Expression of L1 retrotransposons in granulocytes from patients with active systemic lupus erythematosus

Kennedy C. Ukadike[1,2], Rayan Najjar[1], Kathryn Ni[1], Amanda Laine[1], Xiaoxing Wang[1], Alison Bays[1], Martin S. Taylor[3], John LaCava[4,5] and Tomas Mustelin[1*]

Abstract

Background Patients with systemic lupus erythematosus (SLE) have autoantibodies against the L1-encoded open-reading frame 1 protein (ORF1p). Here, we report (i) which immune cells ORF1p emanates from, (ii) which L1 loci are transcriptionally active, (iii) whether the cells express L1-dependent interferon and interferon-stimulated genes, and (iv) the effect of inhibition of L1 ORF2p by reverse transcriptase inhibitors.

Results L1 ORF1p was detected by flow cytometry primarily in SLE $CD66b^{+}CD15^{+}$ regular and low-density granulocytes, but much less in other immune cell lineages. The amount of ORF1p was higher in neutrophils from patients with SLE disease activity index (SLEDAI) > 6 ($p = 0.011$) compared to patients with inactive disease, SLEDAI < 4. Patient neutrophils transcribed seven to twelve human-specific L1 loci (L1Hs), but only 3 that are full-length and with an intact ORF1. Besides serving as a source of detectable ORF1p, the most abundant transcript encoded a truncated ORF2p reverse transcriptase predicted to remain cytosolic, while the two other encoded an intact full-length ORF2p. A number of genes encoding proteins that influence L1 transcription positively or negatively were altered in patients, particularly those with active disease, compared to healthy controls. Components of nucleic acid sensing and interferon induction were also altered. SLE neutrophils also expressed type I interferon-inducible genes and interferon β, which were substantially reduced after treatment of the cells with drugs known to inhibit ORF2p reverse transcriptase activity.

Conclusions We identified L1Hs loci that are transcriptionally active in SLE neutrophils, and a reduction in the epigenetic silencing mechanisms that normally counteract L1 transcription. SLE neutrophils contained L1-encoded ORF1p protein, as well as activation of the type I interferon system, which was inhibited by treatment with reverse transcriptase inhibitors. Our findings will enable a deeper analysis of L1 dysregulation and its potential role in SLE pathogenesis.

Keywords L1, Retrotransposon, Systemic lupus erythematosus, Neutrophils, Interferon

*Correspondence:
Tomas Mustelin
tomas2@uw.edu
Full list of author information is available at the end of the article

Background

Autoantibodies against nucleic acids and proteins associated with them, as well as elevated type I interferons in 60–90% of patients [1–3] are hallmarks of systemic lupus erythematosus (SLE), a systemic and often severe autoimmune disease. We recently reported that a majority of adult [4] and pediatric [5] SLE patients also have autoantibodies against one of the two proteins encoded by the long interspersed element-1 (LINE-1 or L1), termed ORF1p. These autoantibodies are higher in patients with active disease than in those in remission and they correlate positively with many measures of disease activity, such as the SLE disease activity index (SLEDAI), complement consumption, anti-double-stranded DNA antibodies, other autoantibodies, type I interferons, and the presence of lupus nephritis [4, 5].

The L1 retrotransposon has been extraordinarily prolific over evolutionary time: it is present in the genomes of organisms in all kingdoms of life, often in large copy numbers. There are over 500,000 copies of L1 in our own genome, constituting approximately 17% of it [6–8]. L1 sequences are present both within introns of protein-coding genes and in intergenic regions. The vast majority of these L1 sequences are incomplete (most often 5' truncated) and contain numerous mutations that disrupt the two open reading-frames, termed *ORF1* and *ORF2*; these loci cannot produce the encoded proteins or use them to retrotranspose. Only 90 L1 have intact ORFs and 82 are full-length and seemingly intact, but as few as six of them are still 'hot'[9], *i.e.,* these loci are mobile in contemporary humans.

While there is currently no indication that de novo insertions of L1 play any role in SLE or other autoimmune diseases, the L1-encoded proteins have the capacity to cause pathology by other mechanisms [10]. The protein encoded by *ORF2*, termed ORF2p, is an active reverse transcriptase [11, 12], which uses RNA as a template to synthesize a DNA copy of the RNA sequence. The first product is an RNA:DNA heteroduplex; in the canonical L1 lifecycle, this occurs within the nucleus as part of a mechanism termed target-primed reverse transcription [13]. Unexpectedly, both RNA:DNA heteroduplexes and single-stranded DNA have been detected in the cytosol in cells with active L1 [14, 15], indicating that cytosolic reverse transcription also occurs. Furthermore, the synthesized DNA can trigger DNA sensors, such as cyclic-guanine adenosine synthase (cGAS)[16], ZCCHC3 [17, 18], and ZBP1 [19, 20], the physiological functions of which are to detect cytosolic pathogen-derived DNA. It was recently reported [21] that L1 ORF2p-catalyzed reverse transcription, cGAS-mediated DNA-sensing, and the resulting IFNβ production operate during late cellular senescence both in cell culture and in intact mice and, presumably, in humans. The produced IFNβ contributed to the inflammation associated with aging, but was eliminated by reverse transcriptase inhibitors [21].

The polypeptide encoded by *ORF1*, termed ORF1p, is ~ 40 kDa in mass and forms homotrimeric [22, 23] and oligomeric [24] proteins with RNA-binding, nucleic-acid-chaperone properties that coat the L1 RNA; ORF1p is necessary for L1 retrotransposition (reviewed in [25, 26]). ORF1p:ORF2p interactions apparently depend on the presence of intact RNA [18, 27]. Importantly, under ectopic expression in HEK-293 T cells, ORF1p is present in up to ~ tens of copies per ORF2p in affinity-enriched L1 ribonucleoprotein (RNP) [27], but in endogenously expressing cell lines and human cancer tissues [28], the stoichiometry of ORF1p:ORF2p is much higher. Endogenous ORF1p has been shown to accumulate in the cytoplasm [29] and to populate RNA (stress) granules [30]. Studies using ectopic L1 expression have also provided evidence that L1 RNP accumulates within stress granules [30–34]), although alternative characterizations have also been proposed [18, 35]. ORF1p- and L1-related RNPs co-assemble with a diverse range of nucleic acids [18, 35, 36]; the L1 RNA itself exhibits immunogenic viral mimicry [36]. ORF1p- and L1-related RNPs associate with several well-known autoantigens in SLE, such as RO60 [27, 37–39]. SLE patients also have autoantibodies that recognize several of the other cellular proteins that associate with ORF1p in the RNA-rich macromolecular aggregates (manuscript submitted). While ORF1p is not able to drive retrotransposition without the participation of ORF2p, one could envision that ORF1p by virtue of its immunogenicity could play a role in SLE by forming immune complexes with autoantibodies that recognize it [10]. Such immune complexes could be deposited in tissues, such as the kidney, and contribute to the tissue inflammation observed in patients with SLE.

The presence of autoantibodies in SLE patients that react with ORF1p suggests that this protein is, or recently was, expressed in patients. Indeed, it was detected by immunoblotting and immunohistochemistry in salivary glandular cells from a Sjögren's syndrome patient and in a renal biopsy from a lupus nephritis patient [40, 41]. The positive correlation of autoantibodies against ORF1p with disease activity measured by SLEDAI or complement consumption also suggests that the presence of the protein may be specifically associated with active disease. To test this, we analyzed immune cells isolated from the blood of patients with SLE for the presence of ORF1p protein, L1 transcripts, L1 regulators, and reverse transcriptase-dependent IFNβ and IFN-inducible genes pre- and post-treatment with reverse transcriptase inhibitors.

Results

Detection of ORF1p in SLE neutrophils by flow cytometry

To determine if the anti-ORF1p autoantibodies present in SLE patients [4, 5] are matched by the presence of this protein in any of their immune cells, we stained polymorphonuclear (PMN) and peripheral blood mononuclear leukocytes (PBMC) from SLE patients or healthy donors with the anti-ORF1p monoclonal antibody 4H1 and counter-stained them with lineage markers. To prevent non-specific staining, 4H1 was directly conjugated to fluorophore (as were the lineage markers) and all steps of the staining protocol included an unlabeled Fc receptor-blocking antibody and 1% normal mouse serum (all antibodies were mouse antibodies). These precautions will eliminate any binding of labeled antibodies through their Fc portions to surface Fc receptors, which are present on neutrophils. Flow cytometry was performed with all combinations, as well as combinations lacking each individual antibody. As shown in Fig. 1A with a representative patient, 35% of the neutrophils, as identified with the lineage marker CD66b (CEACM8), in the PMN fraction were positive for ORF1p, as were 45% of the neutrophils stained by CD14, which is also a present on most neutrophils. In the PBMC fraction, less than 1% of monocytes or B cells were positive in the shown patient (Fig. 1B).

In a cohort of patients ($n=13$) and healthy donors ($n=5$), 10 patients had ORF1p$^+$ CD66b$^+$ neutrophils with the percentage of positive cells ranging from 3–72% with an average of 20.3% ($\pm$26.9%; $n=13$) (Fig. 1C). The CD66b$^+$ cells in the PBMC fraction, which represent low-density granulocytes (based on their neutrophil marker CD66b and presence in the lower density PBMC fraction) potentially with some contaminating regular granulocytes, also varied from 0–82%. The average was 19.5% ($\pm$25.3%, $n=10$). CD14$^+$ monocytes in the PBMC were positive in 2 patients, CD19$^+$ B cells in 3 patients, and CD3$^+$ T cells in one (Fig. 1C), while these lineages were all negative in heathy donors (Fig. 1D). We noted that the patients with active disease (SLEDAI ≥ 6) had higher percentages of ORF1p$^+$ neutrophils (average 28.6%) than those with low disease activity (SLEDAI ≤ 4) (average 1.7%) at the time of the blood draw ($p=0.011$) (Fig. 1E). This was also true for the low-density granulocytes ($p=0.038$) with averages of 29.3% vs 4.8% (Fig. 1E), while the trend towards a similar difference in B cells (3.8 vs 0.3%) was not statistically significant. A linear regression analysis of this relationship is also shown (Fig. 1F).

Identification of L1Hs loci that are transcriptionally active

To characterize their potential to produce ORF1p, we analyzed L1Hs transcripts in neutrophils from fifteen SLE patients and twelve healthy controls using RNA-seq. This approach has well-known issues with multi-mapping (*i.e.*,150-bp reads may map to more than one genomic locus) – we therefore focused our analyses on L1 sequences that could be uniquely mapped to a single locus ('uniquely mapping'). Of these, transcripts from a total of 36 L1Hs loci were present in the patients and healthy controls combined. This number increased to 71 when multi-mapping reads were included, albeit most of them below our cut-off of 10 read counts at least in one sample. Of the uniquely mapping L1Hs transcripts, 7 were elevated > twofold in SLE neutrophils compared to healthy donor neutrophils (Fig. 2A, Supplemental Fig. S1 and Supplemental Table 1). This number was 12 when reads matching more than one locus were included (Supplemental Fig. S2). Interestingly, each of the SLE patients had a unique pattern of transcripts from these L1Hs loci with a tendency of those with active disease (SLEDAI > 6) to express more loci (Fig. 2B). Of the increased 7 uniquely mapping L1Hs, only 3 originate from full-length (> 6,010 bp) L1Hs loci with a 338-codon *ORF1* without stop codons and therefore potentially able to produce ORF1p (Fig. 2A-E). Segregating the SLE patients by SLEDAI score into active versus inactive disease, or by ISG expression into those with elevated (> 2 SD of healthy donors) versus low ISGs, revealed that L1Hs expression tended to be higher both in active disease and in those patients with elevated ISGs (Fig. 2C, D, E), although this was statistically significant only for the L1Hs on chr4:87,347,104–87,353,146 (Fig. 2C). This was also true for the other 4 elevated L1Hs loci (lacking intact ORF1) (Supplemental Fig. S1). We conclude that the ORF1p that we detect in SLE neutrophils is likely the product of 3 distinct L1Hs loci, the individual contribution of which appear to vary between patients.

(See figure on next page.)

Fig. 1 Presence of L1 ORF1p in neutrophils from SLE patients. **A** Flow cytometry of PMN from a representative SLE patient with active disease stained for ORF1p and the lineage markers CD66b (middle row) and CD14 (bottom row) compared to cells stained with all antibodies except ORF1p (FMO, fluorescence minus one). **B** Flow cytometry of PBMC from the same SLE patient stained for ORF1p and the lineage markers CD19 (middle row) and CD14 (bottom row) compared to FMO controls. **C** Summary of the percent ORF1p + leukocytes in 13 SLE patients: neutrophils (CD66b$^+$ PMN), low-density granulocytes (CD66b$^+$ PBMC), B cells (CD19 + PBMC), T cells (CD3$^+$ PBMC), and monocytes (CD14$^+$ PBMC). Error bars represent standard deviation. **D**. Summary of the percent ORF1p$^+$ leukocytes in 6 healthy controls (HC) in the same cell lineages. **E** The percent ORF1p$^+$ neutrophils (open circles), low-density granulocytes (filled circles), and B cells (filled triangles) in patients with low SLEDAI < 4 ($n=4$; -lo) and patients with high SLEDAI > 6 ($n=9$; -hi). **F** Linear regression analysis of the percentages of ORF1p$^+$ neutrophils (open circles), low-density granulocytes (filled circles), and B cells (filled triangles) versus SLEDAI of each patient

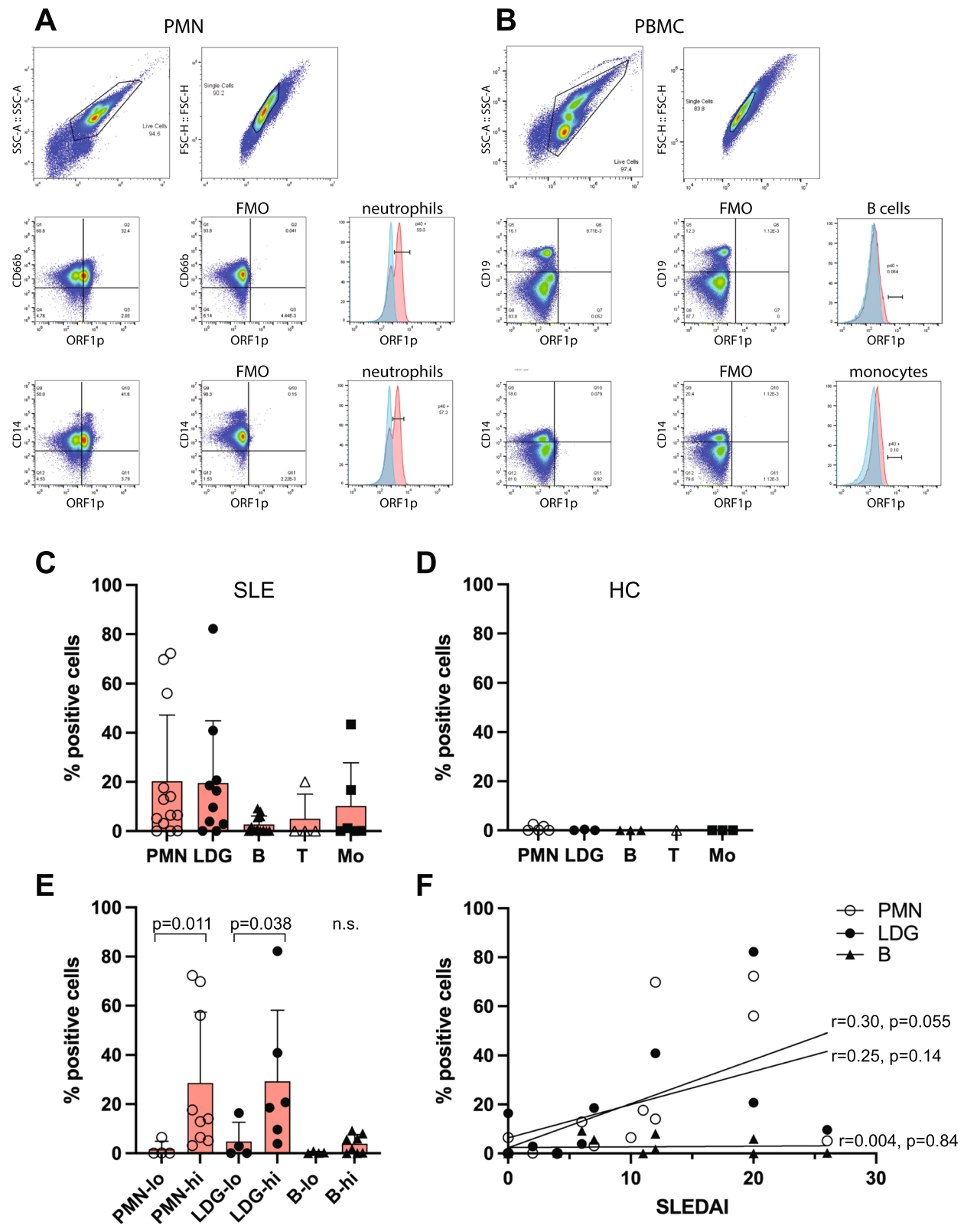

Fig. 1 (See legend on previous page.)

To expand the analysis, we downloaded a publicly available neutrophil RNA-seq dataset (Gene Expression Omnibus database, accession number GSE139360) from SLE patients ($n=30$) and healthy controls ($n=29$). This data set also revealed that L1Hs_chr4:87,347,104–87,353,146 was increased ($p<0.05$) (Fig. 2F), as was L1Hs_chr3:159,095,380–159,101,394, though the latter was not statistically significant not shown).

Regarding the second L1-encoded protein, ORF2p, which is a reverse transcriptase, our data reveal that only three of the transcribed loci have an intact *ORF1* allowing for translation of *ORF2*, but only two of them have these have an intact *ORF2*, namely L1Hs_chr20:12,801,018–12,807,044 (Fig. 2 D) and L1Hs_chr7:113,776,123–113,782,152 (Fig. 2E), while the other 4 transcripts (Supplemental Fig. S1A-D) have stop codons in *ORF2*, lack portions of *ORF2*, or have stop codons in *ORF1* that halt translation before the brief gap that allows ORF2p to be translated from the bicistronic L1 transcript [42]. Interestingly, L1Hs_chr4:87,347,104–87,353,146 has a frame-shift mutation in *ORF2* predicted to result in an 870-residue protein with a short novel C-terminus, rather than the full-length 1275-residue ORF2p. This truncated ORF2p contains the entire reverse-transcriptase domain but lacks the cysteine-rich C-terminal region, which is required for retrotransposition [43], but not required for reverse-transcriptase activity. We speculate that this truncated ORF2p is an active reverse transcriptase, but does not support L1 retrotransposition: it may remain in the cytosol where it can produce interferonogenic DNA products.

Of potential relevance, L1Hs_chr4:87,347,104–87,353,146 maps to cytogenetic band 4q22.1 and is located in the 5th intron of a gene involved in estradiol metabolism, hydroxysteroid 17-beta-dehydrogenase 11 (*HSD17B11*) on the same negative DNA strand (Fig. 2G). Our RNA-seq data showed that *HSD17B11* is expressed in heathy neutrophils and is increased in SLE neutrophils, particularly from patients with active disease (Fig. 2H). Importantly, transcription of the entire *HSD17B11* will not result in translatable L1Hs RNA since the excision of intron 5 during RNA splicing will not result in nuclear export of an L1-containing RNA with a poly-A tail.

Expression of epigenetic and transcriptional regulators of L1

Next, we analyzed the expression of regulators of L1 transcription, RNA decay, and other factors influencing L1 biology. Because ORF1p was present predominantly in neutrophils from SLE patients with active disease, we focused our analysis on the samples from patients with active disease ($n=7$) versus those with inactive disease ($n=8$), as well as the healthy donors ($n=12$). We also segregated all the patients by their expression of interferon-inducible genes (ISGs) into those with low ($n=4$) or high ISGs ($n=11$).

L1 transcription is effectively silenced by DNA methylation catalyzed by DNA methyltransferase 1 (*DNMT1*) and 3A (*DNMT3A*), the expression of which was not significantly altered in SLE neutrophils (Fig. 3A). DNA methylation, in turn, allows for the binding of the Human Silencing Hub (HUSH) complex [44–46], which consists of the proteins encoded by the genes *MPHOSPH8*, *TASOR*, and *PPHLN1*, in conjunction with *SETDB1*, *ATF7IP*, *TRIM28*, the chromatin regulator *MORC2*, and KRAB-domain containing Zinc-finger factors, such as *ZNF765, ZNF528*, and *ZNF141* (for L1Hs). Transcripts for these genes were unchanged in SLE neutrophils compared to neutrophils from healthy donors, except for *TRIM28* which was decreased in a statistically significant manner ($p<0.005$) (Fig. 3A). These data do not reveal any global reduction in these mechanisms of L1 repression, but do not preclude the possible existence of locus-specific alterations.

L1 transcripts are also subject to decay through the action of the nuclear exosome targeting (NEXT[47]) complex (Fig. 3B), which interacts with the HUSH complex. The genes constituting this complex are *ZCCH8*,

(See figure on next page.)

Fig. 2 L1Hs expressed at elevated levels in SLE neutrophils. **A** Average normalized read counts of the transcripts uniquely mapping to full-length L1Hs loci that are increased in neutrophils from SLE patients ($n=15$) and healthy donors (HC; $n=12$). The loci are identified by their chromosomal location and genomic coordinates. **B**. Heat map representation of individual patient patterns of L1Hs expression. The normalized read counts were adjusted to 100 for the highest expression of each locus. **C** The predicted translation products of the indicated L1Hs element on chromosome 4 and the normalized read counts for it in the healthy controls (HC) in the SLE patients segregated by SLEDAI score into low versus high disease activity (left panel) or by low versus high ISG levels (right panel). Red letters 'x' denote premature stop codons, red boxes represent *ORF1* translatable into full-length 338-amino acid residue ORF1p. Purple boxes represent ORF2p; full-length is 1275aa. Note that *ORF2* in this locus has a frame-shift mutation followed by a stop codon that terminates the protein after 870aa residues, which includes intact endonuclease (EN) and reverse transcriptase (RT) domains, but lacks the C-terminal Cys-rich domain (CR), the sequence of which can be found in a different reading frame (pale blue box) and therefore not translated. **D** same data for the indicated L1Hs on chromosome 20, which is full-length and has intact ORF1 and ORF2. **E** Same data for the indicated L1Hs on chromosome 7. **F** Side-by-side data from the present study (left panel) and similarly retrieved data from data set GSE139360 ($n=30$ SLE, $n=29$ HC) for the same L1Hs as in panel C. **G** Schematic illustration of the location of the same L1Hs (chr4:87347104–87353146) within the 5th intron of the *HSD17B11* gene. The L1Hs element must be independently transcribed from its 5' UTR to be poly-adenylated and translated. **H** Normalized read counts for the processed mRNA of HSD17B11 in HC and SLE patients segregated by disease activity. Bars indicate mean ± standard deviation. * denotes p values < 0.05, ** $p<0.01$, and *** $p<0.005$

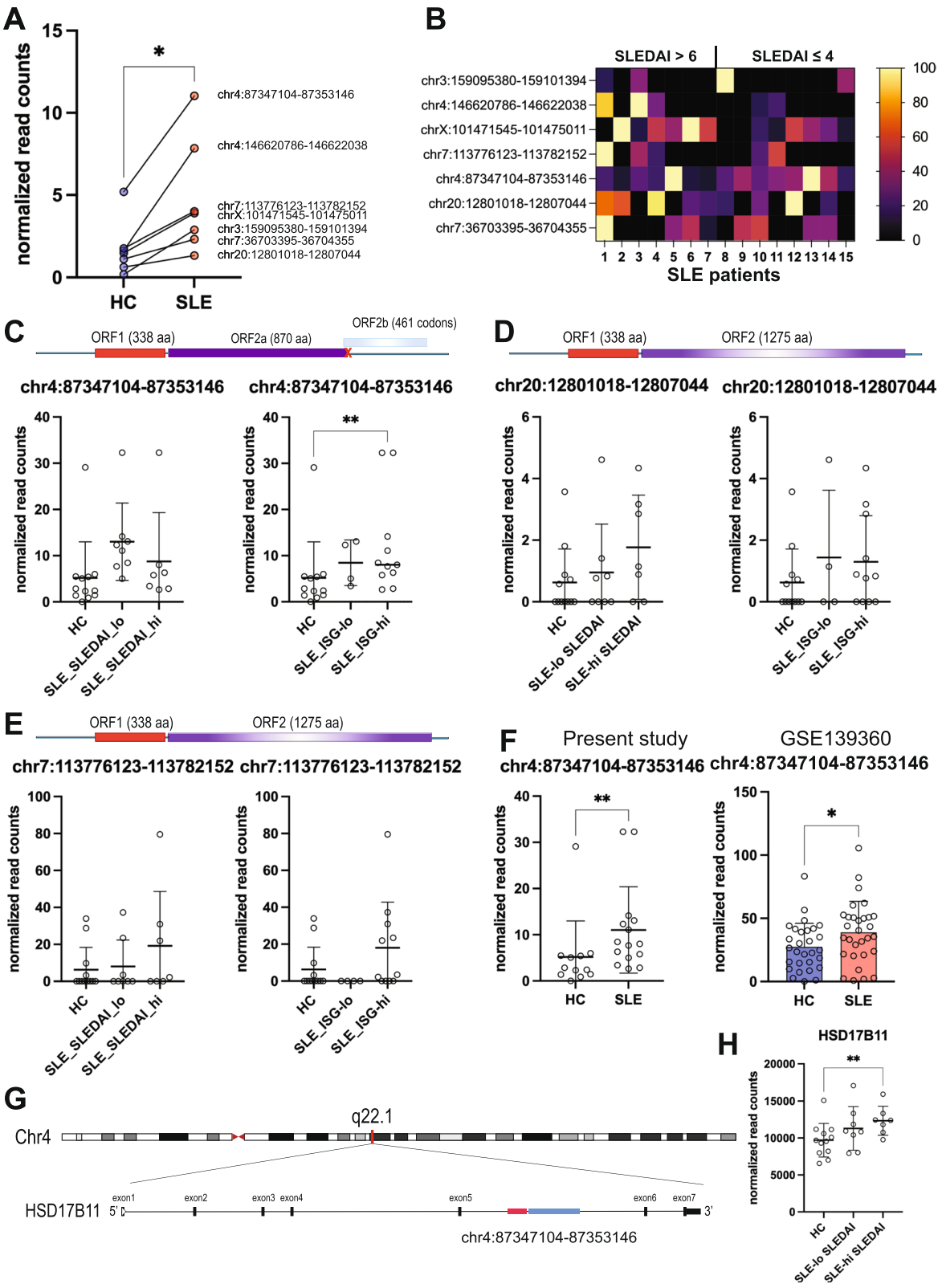

Fig. 2 (See legend on previous page.)

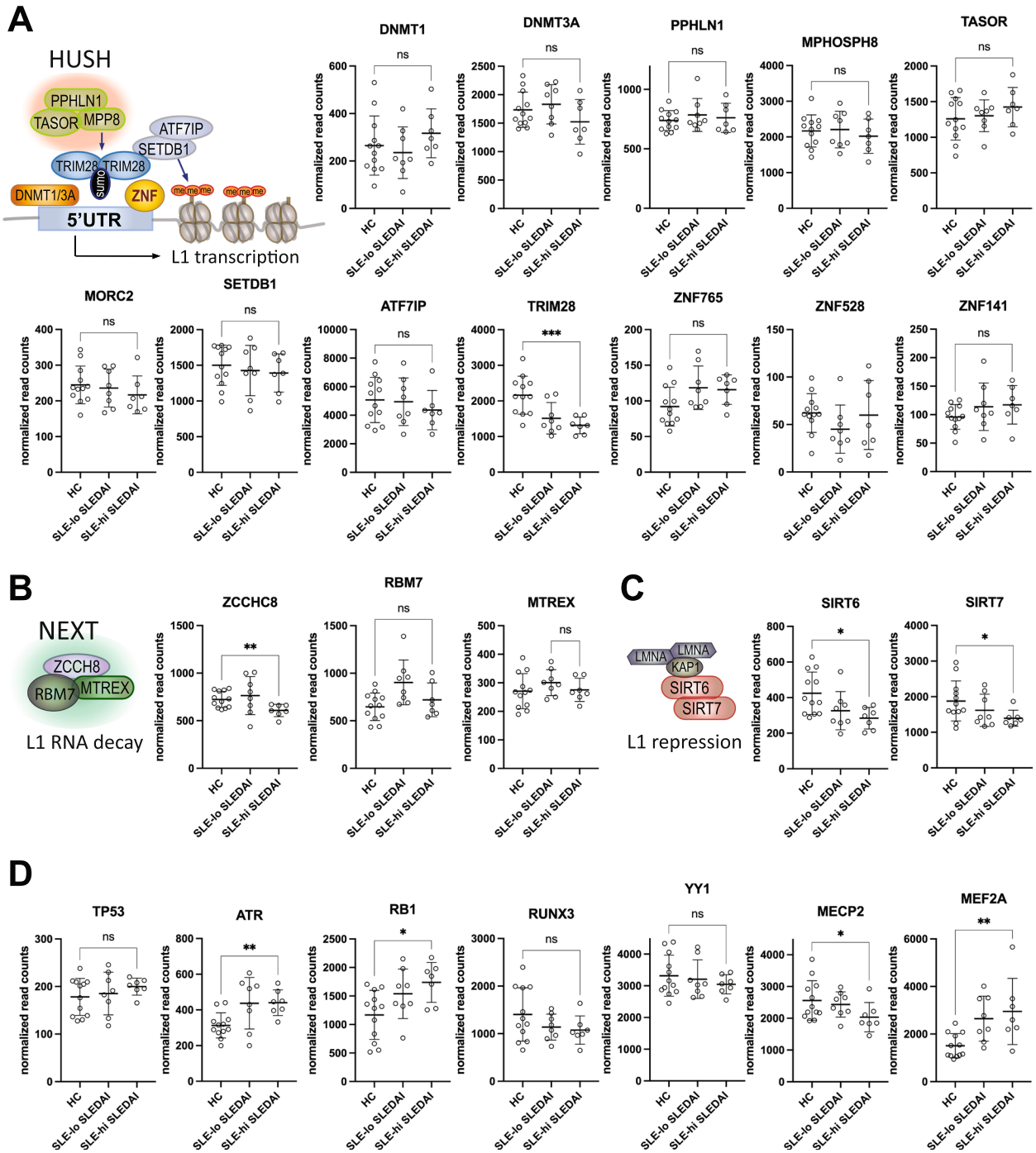

Fig. 3 Expression of genes involved in epigenetic, transcriptional, or post-transcriptional regulation of L1 in neutrophils from SLE patients and healthy volunteers. **A** Schematic representation of the HUSH complex and the proteins involved in silencing L1 loci and expression of the indicated genes in HC and SLE patients segregated by disease activity. **B** Schematic representation of the NEXT complex that regulates L1 transcript decay and expression of the indicated genes in HC and SLE patients. **C** Schematic representation of the sirtuins that maintain inactive heterochromatin structure and anchor L1 loci to lamin A in the inner nuclear envelope and expression of *SIRT6* and *SIRT7* in HC and SLE patient neutrophils. **D** Other known regulators of L1 transcription and the expression these genes in HC and SLE neutrophils. Bars indicate mean ± standard deviation. * denotes p values < 0.05, ** $p < 0.01$, and *** $p < 0.005$

MTREX4, and *RBM7*, of which *ZCCH8* was decreased in neutrophils from active SLE compared to neutrophils from inactive SLE or healthy controls (Fig. 3B). The other genes of the NEXT complex were unchanged. L1 loci are repressed in many cells, in part, by the sirtuins SIRT6[48] and SIRT7[49], which inactivate these loci via the maintenance of repressive heterochromatin anchored to lamin A in the inner nuclear envelope. Interestingly, expression of both *SIRT6* and *SIRT7* were decreased in SLE neutrophils, particularly from those with active disease (Fig. 3C). This may contribute to increased transcription of L1Hs in SLE.

Additional transcription factors or epigenetic modulators reported to regulate L1 expression, were elevated (*ATR*, *RB1*, *MEF2A*) or downregulated (*MECP2*) moderately, reaching statistical significance (Fig. 3D). It is not clear at this time how these alterations would affect L1Hs transcript levels in SLE.

Expression of regulators of L1 biology

The L1-encoded ORF1p and ORF2p proteins exist in cells as macromolecular assemblies with several other RNA-binding proteins, at least some of which influence their activity. Transcripts of *RO60* and *MOV10* were strongly upregulated in SLE neutrophils ($p < 0.001$), while *LARP7* was unchanged (Fig. 4A). This effect was evident in neutrophils from both patients with inactive and active disease (Fig. 4A), but was much more clearly influenced by type I interferons (Fig. 4B).

SLE neutrophils have upregulated nucleic acid-sensors

The expression of many of the genes that encode nucleic acid sensors and components of their signaling to type I interferon production (Fig. 4A) were significantly altered in SLE neutrophils compared to healthy controls: transcripts for the DNA sensors *CGAS* and *ZBP1* and the two RNA sensors RIG-1 (*DDX58*) and MDA5 (*IFIH1*) were significantly increased, as were the transcripts for TBK1 (Fig. 4A), while *DDX41* was downregulated (Fig. 4A). Interestingly, the IRF3 transcription factor was significantly downregulated, while the related IRF5 and IRF7 instead were increased (Fig. 4A).

Because patients with a high type I interferon signature appear to have a molecularly distinct form of SLE, we segregated the patients by interferon signature (i.e. ISG levels > 95 percentile of the healthy control distribution), which revealed a much more pronounced upregulation of the genes that encode nucleic acid sensors and components of their signaling pathway in the ISG-high patients (Fig. 4B). Collectively, these data illustrate an enhanced capacity to recognize pathogenic nucleic acids and drive type I interferon production.

Neutrophils contain reverse transcriptase inhibition-sensitive interferon stimulated genes (ISGs) and IFNβ

To begin to dissect the potential consequences of the expression of intact and functional L1Hs loci in SLE neutrophils, we first measured by real-time PCR a commonly used set of type I interferon-inducible genes (*IFI6, IFI27, IFI44,* and *IFI44L*) in both neutrophils and lymphocytes from SLE patients and heathy volunteers. As expected, some SLE patients expressed these genes at elevated levels, and others at levels comparable to healthy donors (Fig. 5A). Compared to the housekeeping gene *GAPDH*, those SLE patients with elevated expression (often referred to as 'interferon signature positive'), had 2–fourfold higher expression of these genes in their neutrophils (Fig. 5A) compared to their lymphocytes (Fig. 5B). This is also evident when the average value of the 4 ISGs are calculated from each patient (Fig. 5C). Similar results were seen in our RNA-seq data (Fig. 5D): 108 ISGs were increased up to 445-fold in SLE neutrophils compared to healthy donor neutrophils, while these transcripts were 2- to 6.4-fold lower ($p = 0.0045$) in the lymphocytes from the same donors.

A 4-h treatment of SLE neutrophils from three independent donors with the combination of the two reverse transcriptase inhibitors, emtricitabine and tenofovir alafenamide, which are known to be effective against ORF2p [50, 51], resulted in a decline in the ISGs, as well as reduced *IFNB* expression, compared to neutrophils treated for the same time with medium alone (Fig. 5E and F). Cell viability remained high as assessed by Trypan Blue exclusion and expression of the housekeeping gene GAPDH were identical between these samples (panel C in Supplementary Figure S2). We cannot of course exclude the possibility that emtricitabine and tenofovir influenced *IFNB* expression by non-specific effects.

Discussion

Our data show that SLE patients with active disease exhibit elevated levels of L1Hs transcripts and ORF1p protein predominantly in their neutrophils. The set of

(See figure on next page.)

Fig. 4 Expression of genes involved in post-translational regulation of ORF1p and ORF2p or nucleic acid sensing and signaling to type I interferon induction in neutrophils from SLE patients and healthy volunteers. **A** Schematic representation of the molecular machinery upstream and downstream of the L1 proteins and normalized read counts of the indicated genes in HC and SLE patients segregated by disease activity. **B** Normalized read counts of the same genes in HC and SLE patients segregated in interferon gene signature (ISGs). Bars indicate mean ± standard deviation. * denotes p values < 0.05, ** $p < 0.01$, *** $p < 0.005$, and *** $p < 0.001$. ns, not significant

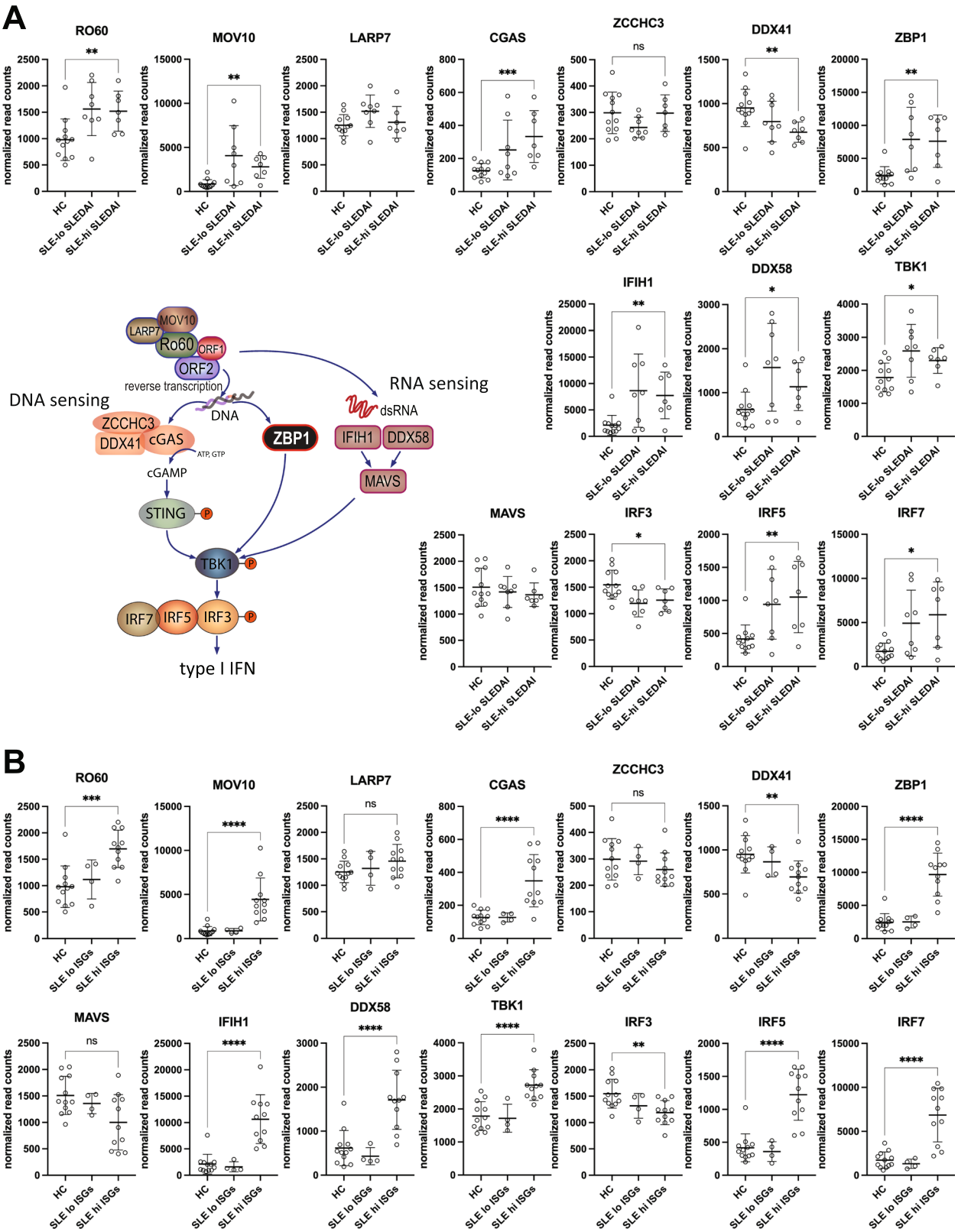

Fig. 4 (See legend on previous page.)

L1Hs loci that are expressed in patient neutrophils differs somewhat between individual patients. In addition, neutrophils from SLE patients as well as from healthy donors contain transcripts from additional L1Hs loci, which are truncated and/or unable to produce ORF1p or ORF2p. Few of these are differentially expressed. There are also transcripts from numerous older L1 families, exceedingly few of which encode intact L1 ORF proteins (and none of which are known to be functional). Our finding that *TRIM28* of the HUSH complex [44–46] is reduced in SLE neutrophils compared to neutrophils from healthy donors could potentially contribute to L1Hs expression. Reduced expression of *SIRT6* and *SIRT7* could also contribute to the higher levels of L1Hs transcripts in SLE, although it is not at this time known if the reduced mRNAs result in reduced levels of SIRT6 and SIRT7 proteins. Polymorphisms in *DNMT1* are also associated with SLE [52] and the gene is reportedly expressed at lower levels in SLE immune cells than in healthy controls [53]. Reduced genomic methylation can also be caused by certain drugs, such as hydralazine and procainamide, which are known to induce SLE (so-called 'drug-induced lupus')[54]. Another well-known trigger of lupus flares, ultraviolet-B light [55], also induces genomic hypomethylation [56]. Our identification of the active L1Hs loci in SLE neutrophils will enable a deeper analysis of their epigenomic landscape, including transcription factors associated with their 5'-untranslated regulatory regions. Furthermore, it should also be stated that detectable ORF1p in SLE neutrophils does not necessarily depend solely on transcription of full-length, intact L1Hs loci. There are reports of translational control of L1 transcripts, for example through its CpG-rich 5'-UTR [57] or microRNAs [58]. Hence, the increased presence of ORF1p in SLE neutrophils could, at least in part, be due to dysregulated translation of L1Hs transcripts or stability of the ORF1p protein.

Another unexpected finding was that the highest abundance, potentially functional L1Hs transcript in SLE neutrophils contained a frame-shift and premature stop codon in *ORF2*. If translated, this would produce an 870-amino acid residue protein with an intact reverse transcriptase domain but lacking the cysteine-rich C-terminal domain; the missing domain is required for retrotransposition, but not for reverse transcriptase activity[50]. We speculate that the truncated ORF2p encoded by the L1Hs at 4q22.1 remains in the cytosol, where it would be well poised to synthesize DNA that triggers cytosolic DNA sensors.

An important finding in our study was that neutrophils from SLE patients also contain higher levels of IFN-inducible gene transcripts than lymphocytes from the same patients. While this could be due to type I IFNs present in the circulation of the patients, the expression of these genes persisted and even increased in the isolated and washed neutrophils over 4 h in culture. Inclusion of the two RTIs, emtricitabine and tenofovir alafenamide, both of which have been shown to inhibit the activity of ORF2p [50, 51], reduced the expression of these IFN-inducible genes. Neutrophils also contained the mRNA for IFNβ, which also declined by approximately half in the presence of these drugs. Unfortunately, neutrophil viability in vitro does not allow for longer incubations. Nevertheless, it seems that cell-intrinsic type I IFN likely contributed to the induction of IFN-response genes and that this cell-intrinsic IFN was dependent on ongoing reverse transcription. L1 ORF2p is also the reverse transcriptase responsible for the aberrant DNA [15, 59] that drives type I IFN production and disease in patients with the interferonopathy Aicardi-Goutières syndrome [60]. In a small clinical trial in these patients, reverse transcriptase inhibition flat-lined the IFN-inducible gene signature for the duration of drug dosing [61].

Conclusions

Our data support a contribution of dysregulated L1Hs expression, translation of L1Hs transcripts, and the biological action of ORF1p and ORF2p to SLE disease. The correlation of SLE disease activity with ORF1p quantity in neutrophils and the presence of reverse transcriptase-sensitive IFN-inducible gene transcripts and IFNβ in these same cells are compatible with a connection between L1 biology and SLE pathogenesis. Ultimately, the importance of L1 dysregulation in SLE pathogenesis will need to be evaluated in a double-blinded

(See figure on next page.)

Fig. 5 RT-sensitive interferon-inducible genes and *IFNB* in neutrophils and lymphocytes from SLE patients and healthy volunteers. **A** Real-time PCR quantitation of four representative interferon-stimulated genes (ISGs) from neutrophils from SLE patients ($n=4$) or HC ($n=1$). The data represent expression normalized by GAPDH signal. **B** Real-time PCR quantitation of the same ISGs from mononuclear cells from SLE patients ($n=4$) or HC ($n=1$). The data represent expression normalized by GAPDH signal. **C** Composite scores (mean) of the same ISGs from neutrophils from SLE patients ($n=14$) or HC ($n=7$). **D** Increased expression of one hundred and eight ISGs identified by RNA-Seq in SLE neutrophils (SLE-PMN) relative to healthy donor neutrophils and in SLE mononuclear cells (SLE-PBMC) relative to healthy donor mononuclear cells. The data points represent the average of each gene among the patients relative to the average expression of the same gene in healthy controls. **E** Real-time PCR quantitation of the ISGs and *IFNB* from neutrophils kept in cell culture for 4 h without or with 10 μM emtricitabine and 1.25 μM tenofovir alafenamide. The data represent the average of 3 independent experiments. **F** The same data as in E shown as individual patients ($n=3$) and as percent of control (100% = without inhibitors)

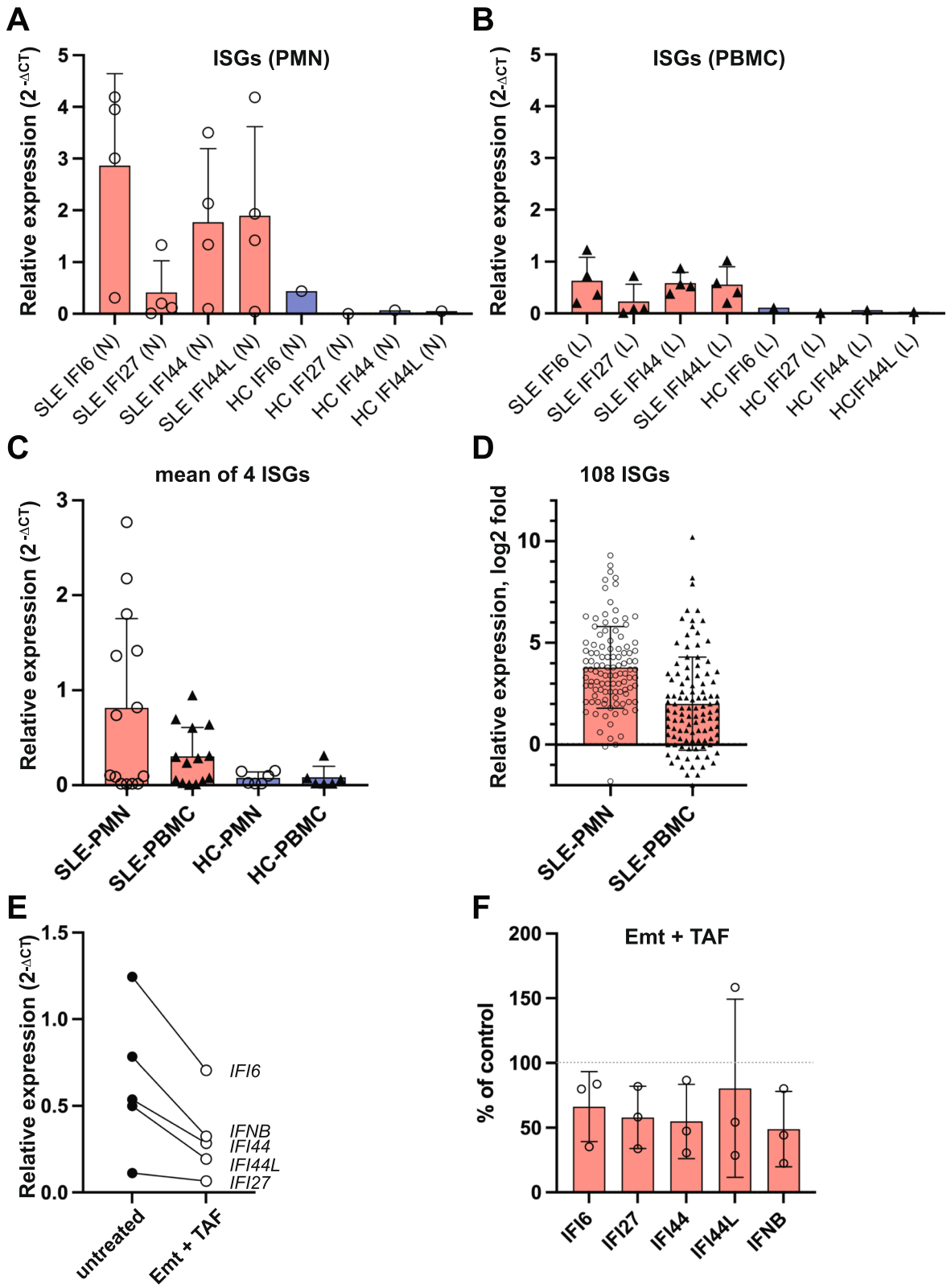

Fig. 5 (See legend on previous page.)

placebo-controlled clinical trial with potent and selective reverse transcriptase inhibitors.

Methods

SLE patients

Freshly drawn blood was obtained from adult patients with SLE and healthy age-matched individuals recruited through the University of Washington, Division of Rheumatology Biorepository to participate in research studies at the University of Washington Medical Center, Seattle, WA. The study was approved by the institutional ethics board (STUDY00006196) and informed written consent was obtained from all participants according to the Declaration of Helsinki.

Isolation of neutrophils and peripheral blood mononuclear cells

Polymorphonuclear (PMN) and peripheral blood mononuclear cells (PBMC) were isolated simultaneously from freshly drawn venous blood by gradient centrifugation on PolymorphPrep according to the manufacturer's instructions. The PMN fraction was > 95% $CD66b^+$ and > 85% $CD15^+$. The majority of PBMC were CD3 + T cells, plus 5–15% $CD19^+$ B cells, 2–6% $CD14^+$ monocytes, and 3–10% $CD66b^+$ low-density granulocytes. The cells were washed and suspended in Hanks' buffered salt solution at a range of $1–10 \times 10^6$ cells/ml before use in various experiments.

Flow cytometry

Cells were stained with anti-CD66 (eBioscience), anti-CD14 (BioLegend), and anti-CD19 (Biolegend) antibodies covalently labeled with PE-Cyanine7, PerCP-Cyanine5.5, and APC-Cyanine7, respectively. Following fixation with 1% paraformaldehyde in phosphate-buffered saline and permeabilization with saponin, cells were stained with an anti-ORF1p antibody 4H1 [27] (MilliporeSigma) covalently labeled with Cy5. An unlabeled blocking antibody to FcγRIIA (CD32A) (Sino Biological Inc.) was also added at this step. After a 1 h incubation, the cells were washed and resuspended in phosphate-buffered saline with saponin and added to a 96-well plate at 1 million cells in 100 µl per well. All steps were performed in the presence of 1% mouse serum to block non-specific binding. Flow cytometry was run on a CytoFLEX Flow Cytometer (Beckman Coulter) and data analysis was done with FlowJo (Becton, Dickinson and Company). FMO (fluorescence minus one) wells were used to determine the cut-off point between background fluorescence and positive populations. Compensation runs were also performed to address any potential overlap of fluorophore emission. Such runs were done with UltraComp eBeads Plus compensation beads (ThermoFisher Scientific).

Treatment of neutrophils with reverse transcriptase inhibitors

Cells were resuspended at 5×10^6 cells in 1 ml of RPMI media containing 10% fetal bovine serum and 1 × Penicillin–Streptomycin in 12-well cell culture plates. Two reverse transcriptase inhibitors (RTIs), emtricitabine (Emt) and tenofovir alafenamide (TAF), were added to the experimental cultures at a final concentration of 10 µM and 1.25 µM, respectively. Note that these are at a ratio of 1:8 based on their therapeutic dose ratio in the combination drug, Descovy® (Emt 200 mg/TAF 25 mg), which is FDA approved for the treatment of HIV infection. The experimental (treated) and control (untreated) cell cultures were then incubated at 37 °C with 5% CO_2 for 4 h before harvesting for RNA extraction.

RNA isolation

Extraction of RNA was performed by using a hybrid protocol of Trizol Reagent (Invitrogen cat# 15,596,026) and RNeasy Micro Kit (Qiagen cat. no. 74004). Cells were lysed and homogenized with Trizol Reagent followed by addition of chloroform to separate DNA and proteins from the RNA to which β-mercaptoethanol was added for additional RNase inhibition. The RNA was precipitated with 70% ethanol, passed through a RNeasy MinElute spin column, and treated with DNase I on the column. The spin column was subsequently washed extensively with the kit-supplied wash buffers, followed by additional conditioning with 70% ethanol before eluting the RNA with RNase-free water.

Real-time quantitative polymerase chain reaction (PCR)

A two-step reverse transcriptase (RT)-quantitative PCR method was utilized by first performing cDNA synthesis using Qiagen QuantiTect Reverse Transcription kit with integrated removal of genomic DNA contamination (Qiagen cat# 205,313) and ran on Applied Biosystems PCR Thermal Cycler. The resultant cDNA was subsequently used as a template for the qPCR setup using the Qiagen QuantiTect SYBR Green PCR kit (Qiagen cat# 204,143) and ran on Applied Biosystems StepOne Plus Real-Time PCR Thermal Cycler. The qPCR incorporated ROX dye as a passive reference to normalize for minor variations in fluorescent intensity between reactions, and GAPDH was used as the housekeeping gene. The relative expressions of L1, *HSD17B11*, and IFN inducible genes were calculated using the $2^{-\Delta CT'}$ method (for non-drug-treated samples) and the $2^{-\Delta\Delta CT}$ method (for drug-treated samples) with normalizations against GAPDH. The following primers were used: *L1* forward 5'-ACCAAAAGTAGA

TAAAACCACAAAGA-3', reverse 5'-GAACTGCGT TCCTTTGGAGG-3' (amplicon 102 bp); *HSD17B11* forward 5'-ACATGTCTGTGTCCTAATTTCGT-3', reverse 5'-TCCCATGCATCAGCCTGTTT-3' (amplicon 109 bp); *IFNB* forward 5'-ACGCCGCATTGACCATCTAT-3', reverse 5'-GTCTCATTCCAGCCAGTGCT-3' (amplicon 85 bp). Primer sequences from Ward et al. [62]: *IFI6* forward 5'-TGCTACCTGCTGCTCTTCA-3', reverse 5'-TCAGGGCCTTCCAGAACC-3' (amplicon 97 bp), *IFI27* forward 5'-TTGTGGCTACTCTGCAGTCA-3', reverse 5'-CCCAGGATGAACTTGGTCAA-3' (amplicon 64 bp); *IFI44* forward 5'-GGCTTTGGTGGGCAC TAATA-3', reverse 5'-TGCCATCTTTCCCGTCTCTA-3' (amplicon 77 bp); *IFI44L* forward 5'-GCAAAAGTGAAG CAAGTTCACA-3', reverse 5'-GAACCTCACTGCAAT CATCCA-3' (amplicon 91 bp).

RNA sequencing and bioinformatics analysis of L1Hs and epigenetic factors

RNA concentration and purity were determined by checking their spectrophotometric absorbances at A260/A280 using BioTek Take3 microplate reader. RNA integrity was verified by performing nondenaturing gel electrophoresis on 1% agarose gel to confirm the presence of the 28S and 18S rRNAs. RNA library preparation was performed using oligo dT selection. Paired-end strand-specific RNA sequencing libraries were generated. Sequences were aligned to the hg38 genome with the STAR aligner [63] TElocal which is part of the TEtranscripts [64] package was used to estimate loci-specific LINE-1 read counts, first time counting only uniquely mapped elements and a second time allowing multimappers. Since younger families of L1HS have accumulated less mutations than older ones, they are more likely to be very similar to each other resulting in multimapping. The DNA sequence for the LINE-1 locus at 4q22.1 (chr4:87,347,104–87,353,146) as annotated by the RepeatMasker database (Smit AFA, Hubley R, and Green P. RepeatMasker Open-3.0. http://www.repeatmasker.org. 1996–2010) was obtained from the UCSC browser [65]. DESeq2 [66] was used to normalize counts and to perform differential gene testing. Reported p values were adjusted for multiple comparisons. Read counts < 10 were excluded from L1Hs analysis. All RNAseq data will be deposited in GEO.

Patient demographics for the RNAseq cohort

The SLE patients ($n=15$) included in the RNA sequencing data set consisted of 13 female and 2 male patients, age 22–74, and white ($n=5$), hispanic ($n=5$), native American ($n=1$), Asian ($n=3$), or black ($n=1$). Two had verified lupus nephritis. They had SLEDAI scores 8–19 ($n=7$) or 0–4 ($n=8$), denoted as active disease and inactive disease, respectively. As determined by having an average expression of 108 ISGs higher than the 95 percentile of the same genes in healthy controls, patients were divided into ISG-high ($n=11$) versus ISG-low ($n=4$). The healthy controls ($n=12$) were sex (3 males, 9 females) and age (23–63) matched and did not have a rheumatic disease.

Statistical analysis

The statistical significance of non-parametric data set from patient samples was calculated using the Mann–Whitney U-test. A p-value < 0.05 was used as the cut-off for statistical significance; values < 0.05 are denoted with *, < 0.01 with **, < 0.005 with ***, and < 0.001 with ****. GraphPad Prism 9.5.0 was used for all statistical analyses.

Supplementary Information

The online version contains supplementary material available at https://doi.org/10.1186/s13100-023-00293-7.

Additional file 1: Supplemental Fig. S1. Expression of the other 4 L1Hs transcripts that are increased in neutrophils from SLE patients. **A** The predicted lack of translation products from the indicated L1Hs element on chromosome 4 and the normalized read counts for its transcript in the healthy controls (HC) in the SLE patients segregated by SLEDAI score into low versus high disease activity (left panel) or by low versus high ISG levels (right panel). **B** Same for the indicated L1Hs on chromosome X. Note that the L1 transcript is bicistronic: ORF2 can only be translated if ORF1 is translated to its end. **C** Same for the indicated L1Hs on chromosome 3. **D** Same for the indicated L1Hs on chromosome 7. Note that this locus is truncated to only the C-terminus of ORF2, which is not likely translated at all. Pale blue boxes are portions of ORF2 that are not translated; full-length is 1275 codons. Red letters 'x' denote premature stop codons. Pink boxes denote truncated ORF1. Domains of ORF2 are the endonuclease (EN), reverse transcriptase (RT), and C-terminal Cys-rich domain (CR).

Additional file 2: Supplemental Fig. S2. Expression of the 12 L1Hs transcripts that are increased in neutrophils from SLE patients using the less stringent approach of allowing for reads that map to more than one genomic location (because they are identical over the 150 bp reads). **A** Heat map representation of individual patient patterns of expression of the 12 L1Hs. The normalized read counts were adjusted to 100 for the highest expression of each locus. **B** The normalized read counts for the additional loci (compared to Fig. 2) in the healthy controls (HC) in the SLE patients segregated by SLEDAI score into low versus high disease activity (left panel) or by low versus high ISG levels (right panel). **C** Individual GAPDH house-keeping gene values as C^T from the real-time PCR reaction with HC or SLE neutrophils treated with medium alone (no drug) or with 10 μM emtricitabine and 1.25 μM tenofovir alafenamide for 4 h (drug) as in Fig. 5E and F.

Additional file 3: Supplemental Table 1. Individual uniquely mapping read counts of the 7 L1 elements expressed at elevated levels in SLE patients.

Acknowledgements

We thank the patients who participated in this study.

Authors' contributions

KCU, MST, JLC, and TM conceived of and designed the study. KCU, RN, KN, AL, XW, AB, generated the data. KCU, RN, AB, MST, JLC, and TM contributed to the analysis and interpretation of data. TM wrote the first version of the manuscript and prepared the figures. All authors contributed to the writing of the

manuscript and to its intellectual content. The author(s) read and approved the final manuscript.

Funding
This work was supported by NIH grants AR075134, AR077266, and AR081654 (to T.M.), T32 AR007108 (to K.U and R.N.), R01GM126170 (to J.L.).

Availability of data and materials
All data will be made available to qualified researchers upon request. The data in the Gene Expression Omnibus database can be retrieved through accession number GSE139360.

Declarations

Ethics approval and consent to participate
The study was approved by the institutional ethics board (STUDY00006196) and informed written consent was obtained from all participants according to the Declaration of Helsinki.

Consent for publication
Not applicable.

Competing interests
TM reports consulting fees from Cugene, QiLu Biopharma, Miro Bio, and Rome Therapeutics. JL has equity in Rome Therapeutics and Oncolinea. MT also has equity in Rome Therapeutics.

Author details
[1]Department of Medicine, Division of Rheumatology, University of Washington, 750 Republican Street, Room E507, Seattle, WA 99108, USA. [2]Department of Internal Medicine, Renown Rheumatology, Renown Health – University of Nevada, Reno School of Medicine, 75 Pringle Way, Suite 701, Reno, NV 89502, USA. [3]Department of Pathology, Massachusetts General Hospital, Boston, MA, USA. [4]Laboratory of Cellular and Structural Biology, The Rockefeller University, New York, NY, USA. [5]European Research Institute for the Biology of Ageing, University Medical Center Groningen, Groningen, The Netherlands.

Received: 29 January 2023 Accepted: 4 May 2023
Published online: 10 May 2023

References

1. Baechler EC, Batliwalla FM, Karypis G, Gaffney PM, Ortmann WA, Espe KJ, et al. Interferon-inducible gene expression signature in peripheral blood cells of patients with severe lupus. Proc Natl Acad Sci U S A. 2003;100(5):2610–5.
2. Bennett L, Palucka AK, Arce E, Cantrell V, Borvak J, Banchereau J, et al. Interferon and granulopoiesis signatures in systemic lupus erythematosus blood. J Exp Med. 2003;197(6):711–23.
3. Crow MK, Kirou KA, Wohlgemuth J. Microarray analysis of interferon-regulated genes in SLE. Autoimmunity. 2003;36(8):481–90.
4. Carter V, LaCava J, Taylor MS, Liang SY, Mustelin C, Ukadike KC, et al. High prevalence and disease correlation of autoantibodies against p40 encoded by long interspersed nuclear elements in systemic lupus erythematosus. Arthritis Rheumatol. 2020;72(1):89–99.
5. Ukadike KC, Ni K, Wang X, Taylor MS, LaCava J, Pachman LM, et al. IgG and IgA autoantibodies against L1 ORF1p expressed in granulocytes correlate with granulocyte consumption and disease activity in pediatric systemic lupus erythematosus. Arthritis Res Ther. 2021;23(1):153.
6. Lander ES, Linton LM, Birren B, Nusbaum C, Zody MC, Baldwin J, et al. Initial sequencing and analysis of the human genome. Nature. 2001;409(6822):860–921.
7. Esnault C, Maestre J, Heidmann T. Human LINE retrotransposons generate processed pseudogenes. Nat Genet. 2000;24(4):363–7.
8. Ostertag EM, Kazazian HH Jr. Biology of mammalian L1 retrotransposons. Annu Rev Genet. 2001;35:501–38.
9. Brouha B, Schustak J, Badge RM, Lutz-Prigge S, Farley AH, Moran JV, et al. Hot L1s account for the bulk of retrotransposition in the human population. Proc Natl Acad Sci U S A. 2003;100(9):5280–5.
10. Ukadike KC, Mustelin T. Implications of endogenous retroelements in the etiopathogenesis of systemic lupus erythematosus. J Clin Med. 2021;10(4):856.
11. Mathias SL, Scott AF, Kazazian HH Jr, Boeke JD, Gabriel A. Reverse transcriptase encoded by a human transposable element. Science. 1991;254(5039):1808–10.
12. Clements AP, Singer MF. The human LINE-1 reverse transcriptase:effect of deletions outside the common reverse transcriptase domain. Nucleic Acids Res. 1998;26(15):3528–35.
13. Luan DD, Korman MH, Jakubczak JL, Eickbush TH. Reverse transcription of R2Bm RNA is primed by a nick at the chromosomal target site: a mechanism for non-LTR retrotransposition. Cell. 1993;72(4):595–605.
14. Thomas CA, Tejwani L, Trujillo CA, Negraes PD, Herai RH, Mesci P, et al. Modeling of TREX1-dependent autoimmune disease using human stem cells highlights L1 Accumulation as a Source of Neuroinflammation. Cell Stem Cell. 2017;21(3):319-31 e8.
15. Lim YW, Sanz LA, Xu X, Hartono SR, Chedin F. Genome-wide DNA hypomethylation and RNA:DNA hybrid accumulation in Aicardi-Goutieres syndrome. Elife. 2015;4:e08007.
16. Gao D, Li T, Li XD, Chen X, Li QZ, Wight-Carter M, et al. Activation of cyclic GMP-AMP synthase by self-DNA causes autoimmune diseases. Proc Natl Acad Sci U S A. 2015;112(42):E5699–705.
17. Lian H, Wei J, Zang R, Ye W, Yang Q, Zhang XN, et al. ZCCHC3 is a co-sensor of cGAS for dsDNA recognition in innate immune response. Nat Commun. 2018;9(1):3349.
18. Taylor MS, Altukhov I, Molloy KR, Mita P, Jiang H, Adney EM, et al. Dissection of affinity captured LINE-1 macromolecular complexes. Elife. 2018;7:e30094.
19. Jiao H, Wachsmuth L, Kumari S, Schwarzer R, Lin J, Eren RO, et al. Z-nucleic-acid sensing triggers ZBP1-dependent necroptosis and inflammation. Nature. 2020;580(7803):391–5.
20. Kuriakose T, Kanneganti TD. ZBP1: Innate Sensor Regulating Cell Death and Inflammation. Trends Immunol. 2018;39(2):123–34.
21. De Cecco M, Ito T, Petrashen AP, Elias AE, Skvir NJ, Criscione SW, et al. L1 drives IFN in senescent cells and promotes age-associated inflammation. Nature. 2019;566(7742):73–8.
22. Khazina E, Weichenrieder O. Human LINE-1 retrotransposition requires a metastable coiled coil and a positively charged N-terminus in L1ORF1p. Elife. 2018;7:e34960.
23. Khazina E, Truffault V, Buttner R, Schmidt S, Coles M, Weichenrieder O. Trimeric structure and flexibility of the L1ORF1 protein in human L1 retrotransposition. Nat Struct Mol Biol. 2011;18(9):1006–14.
24. Callahan KE, Hickman AB, Jones CE, Ghirlando R, Furano AV. Polymerization and nucleic acid-binding properties of human L1 ORF1 protein. Nucleic Acids Res. 2012;40(2):813–27.
25. Martin SL. The ORF1 protein encoded by LINE-1: structure and function during L1 retrotransposition. J Biomed Biotechnol. 2006;2006(1):45621.
26. Martin SL. Nucleic acid chaperone properties of ORF1p from the non-LTR retrotransposon, LINE-1. RNA Biol. 2010;7(6):706–11.
27. Taylor MS, LaCava J, Mita P, Molloy KR, Huang CR, Li D, et al. Affinity proteomics reveals human host factors implicated in discrete stages of LINE-1 retrotransposition. Cell. 2013;155(5):1034–48.
28. Dai L, LaCava J, Taylor MS, Boeke JD. Expression and detection of LINE-1 ORF-encoded proteins. Mob Genet Elements. 2014;4:e29319.
29. Hohjoh H, Singer MF. Cytoplasmic ribonucleoprotein complexes containing human LINE-1 protein and RNA. EMBO J. 1996;15(3):630–9.
30. Goodier JL, Zhang L, Vetter MR, Kazazian HH Jr. LINE-1 ORF1 protein localizes in stress granules with other RNA-binding proteins, including components of RNA interference RNA-induced silencing complex. Mol Cell Biol. 2007;27(18):6469–83.
31. Doucet AJ, Hulme AE, Sahinovic E, Kulpa DA, Moldovan JB, Kopera HC, et al. Characterization of LINE-1 ribonucleoprotein particles. PLoS Genet. 2010;6(10):e1001150.
32. Goodier JL, Mandal PK, Zhang L, Kazazian HH Jr. Discrete subcellular partitioning of human retrotransposon RNAs despite a common mechanism of genome insertion. Hum Mol Genet. 2010;19(9):1712–25.
33. Goodier JL, Cheung LE, Kazazian HH Jr. Mapping the LINE1 ORF1 protein interactome reveals associated inhibitors of human retrotransposition. Nucleic Acids Res. 2013;41(15):7401–19.

34. Hu S, Li J, Xu F, Mei S, Le Duff Y, Yin L, et al. SAMHD1 Inhibits LINE-1 Retrotransposition by Promoting Stress Granule Formation. PLoS Genet. 2015;11(7):e1005367.
35. Briggs EM, McKerrow W, Mita P, Boeke JD, Logan SK, Fenyo D. RIP-seq reveals LINE-1 ORF1p association with p-body enriched mRNAs. Mob DNA. 2021;12(1):5.
36. Šulc P DGA, Solovyov A, Marhon SA, Sun S, Lindholm HT, Chen R, Hosseini A, Jiang H, Ly B-H, Mehdipour P, Abdel-Wahab O, Vabret N, LaCava J, De Carvalho DD, Monasson R, Cocco S, Greenbaum BD. Repeats Mimic Pathogen-Associated Patterns Across a Vast Evolutionary Landscape. BioRxiv. 2023. https://doi.org/10.1101/2021.11.04.467016.
37. Deshmukh US, Lewis JE, Gaskin F, Dhakephalkar PK, Kannapell CC, Waters ST, et al. Ro60 peptides induce antibodies to similar epitopes shared among lupus-related autoantigens. J Immunol. 2000;164(12):6655–61.
38. Menendez A, Gomez J, Caminal-Montero L, Diaz-Lopez JB, Cabezas-Rodriguez I, Mozo L. Common and specific associations of anti-SSA/Ro60 and anti-Ro52/TRIM21 antibodies in systemic lupus erythematosus. ScientificWorldJournal. 2013;2013:832789.
39. Hung T, Pratt GA, Sundararaman B, Townsend MJ, Chaivorapol C, Bhangale T, et al. The Ro60 autoantigen binds endogenous retroelements and regulates inflammatory gene expression. Science. 2015;350(6259):455–9.
40. Mavragani CP, Nezos A, Sagalovskiy I, Seshan S, Kirou KA, Crow MK. Defective regulation of L1 endogenous retroelements in primary Sjogren's syndrome and systemic lupus erythematosus: Role of methylating enzymes. J Autoimmun. 2018;88:75–82.
41. Mavragani CP, Sagalovskiy I, Guo Q, Nezos A, Kapsogeorgou EK, Lu P, et al. Expression of Long Interspersed Nuclear Element 1 Retroelements and Induction of Type I Interferon in Patients With Systemic Autoimmune Disease. Arthritis Rheumatol. 2016;68(11):2686–96.
42. Alisch RS, Garcia-Perez JL, Muotri AR, Gage FH, Moran JV. Unconventional translation of mammalian LINE-1 retrotransposons. Genes Dev. 2006;20(2):210–24.
43. Adney EM, Ochmann MT, Sil S, Truong DM, Mita P, Wang X, et al. Comprehensive Scanning Mutagenesis of Human Retrotransposon LINE-1 Identifies Motifs Essential for Function. Genetics. 2019;213(4):1401–14.
44. Robbez-Masson L, Tie CHC, Conde L, Tunbak H, Husovsky C, Tchasovnikarova IA, et al. The HUSH complex cooperates with TRIM28 to repress young retrotransposons and new genes. Genome Res. 2018;28(6):836–45.
45. Tunbak H, Enriquez-Gasca R, Tie CHC, Gould PA, Mlcochova P, Gupta RK, et al. The HUSH complex is a gatekeeper of type I interferon through epigenetic regulation of LINE-1s. Nat Commun. 2020;11(1):5387.
46. Garland W, Muller I, Wu M, Schmid M, Imamura K, Rib L, et al. Chromatin modifier HUSH co-operates with RNA decay factor NEXT to restrict transposable element expression. Mol Cell. 2022;82(9):1691–707 e8.
47. Lubas M, Christensen MS, Kristiansen MS, Domanski M, Falkenby LG, Lykke-Andersen S, et al. Interaction profiling identifies the human nuclear exosome targeting complex. Mol Cell. 2011;43(4):624–37.
48. Van Meter M, Kashyap M, Rezazadeh S, Geneva AJ, Morello TD, Seluanov A, et al. SIRT6 represses LINE1 retrotransposons by ribosylating KAP1 but this repression fails with stress and age. Nat Commun. 2014;5:5011.
49. Vazquez BN, Thackray JK, Simonet NG, Chahar S, Kane-Goldsmith N, Newkirk SJ, et al. SIRT7 mediates L1 elements transcriptional repression and their association with the nuclear lamina. Nucleic Acids Res. 2019;47(15):7870–85.
50. Dai L, Huang Q, Boeke JD. Effect of reverse transcriptase inhibitors on LINE-1 and Ty1 reverse transcriptase activities and on LINE-1 retrotransposition. BMC Biochem. 2011;12:18.
51. Jones RB, Garrison KE, Wong JC, Duan EH, Nixon DF, Ostrowski MA. Nucleoside analogue reverse transcriptase inhibitors differentially inhibit human LINE-1 retrotransposition. PLoS One. 2008;3(2):e1547.
52. Park BL, Kim LH, Shin HD, Park YW, Uhm WS, Bae SC. Association analyses of DNA methyltransferase-1 (DNMT1) polymorphisms with systemic lupus erythematosus. J Hum Genet. 2004;49(11):642–6.
53. Nawrocki MJ, Majewski D, Puszczewicz M, Jagodzinski PP. Decreased mRNA expression levels of DNA methyltransferases type 1 and 3A in systemic lupus erythematosus. Rheumatol Int. 2017;37(5):775–83.
54. Cornacchia E, Golbus J, Maybaum J, Strahler J, Hanash S, Richardson B. Hydralazine and procainamide inhibit T cell DNA methylation and induce autoreactivity. J Immunol. 1988;140(7):2197–200.
55. Lieberman MW, Beach LR, Palmiter RD. Ultraviolet radiation-induced metallothionein-I gene activation is associated with extensive DNA demethylation. Cell. 1983;35(1):207–14.
56. Wu Z, Li X, Qin H, Zhu X, Xu J, Shi W. Ultraviolet B enhances DNA hypomethylation of CD4+ T cells in systemic lupus erythematosus via inhibiting DNMT1 catalytic activity. J Dermatol Sci. 2013;71(3):167–73.
57. Dmitriev SE, Andreev DE, Terenin IM, Olovnikov IA, Prassolov VS, Merrick WC, et al. Efficient translation initiation directed by the 900-nucleotide-long and GC-rich 5′untranslated region of the human retrotransposon LINE-1 mRNA is strictly cap dependent rather than internal ribosome entry site mediated. Mol Cell Biol. 2007;27(13):4685–97.
58. Ohms S, Lee SH, Rangasamy D. LINE-1 retrotransposons and let-7 miRNA: partners in the pathogenesis of cancer? Front Genet. 2014;5:338.
59. Li P, Du J, Goodier JL, Hou J, Kang J, Kazazian HH Jr, et al. Aicardi-Goutieres syndrome protein TREX1 suppresses L1 and maintains genome integrity through exonuclease-independent ORF1p depletion. Nucleic Acids Res. 2017;45(8):4619–31.
60. Keating SE, Baran M, Bowie AG. Cytosolic DNA sensors regulating type I interferon induction. Trends Immunol. 2011;32(12):574–81.
61. Rice GI, Meyzer C, Bouazza N, Hully M, Boddaert N, Semeraro M, et al. Reverse-Transcriptase Inhibitors in the Aicardi-Goutieres Syndrome. N Engl J Med. 2018;379(23):2275–7.
62. Ward JM, Ratliff ML, Dozmorov MG, Wiley G, Guthridge JM, Gaffney PM, et al. Expression and methylation data from SLE patient and healthy control blood samples subdivided with respect to ARID3a levels. Data Brief. 2016;9:213–9.
63. Dobin A, Davis CA, Schlesinger F, Drenkow J, Zaleski C, Jha S, et al. STAR: ultrafast universal RNA-seq aligner. Bioinformatics. 2013;29(1):15–21.
64. Jin Y, Tam OH, Paniagua E, Hammell M. TEtranscripts: a package for including transposable elements in differential expression analysis of RNA-seq datasets. Bioinformatics. 2015;31(22):3593–9.
65. Kent WJ, Sugnet CW, Furey TS, Roskin KM, Pringle TH, Zahler AM, et al. The human genome browser at UCSC. Genome Res. 2002;12(6):996–1006.
66. Love MI, Huber W, Anders S. Moderated estimation of fold change and dispersion for RNA-seq data with DESeq2. Genome Biol. 2014;15(12):550.

Publisher's Note